49	Ma E, Iwasaki M, et al.	Dietary intake of folate, vitamin B2, vitamin B6, vitamin B12, genetic polymorphism of related enzymes, and risk of breast cancer: a case-control study in Japan	Nutr Cancer	61(4)	447-456	2009
50	Hasebe T, Iwasaki M, et al.	p53 expression in tumor-stromal fibroblasts is closely associated with the nodal metastasis and outcome of patients with invasive ductal carcinoma who received neoadjuvant therapy	Hum Pathol	2009 Oct 14. [Epub ahead of print]		
51	Gotoda T, Iwasaki M, et al.	Retrospective comparative study on clinical outcome of endoscopic resection of early gastric cancer treated by traditional and expanded National Cancer Center (NCC) criteria	Br J Surg	(in press)		
52	Nakazato T, Bono H, et al.	Gendoo: functional profiling of gene and disease features using MeSH vocabulary	Nucleic Acids Res	2009 Jul 1;37(Web Server issue):W166-9. Epub 2009 Jun 4.		

Biochemical and Biophysical Research Communications 394 (2010) 303–308

Contents lists available at ScienceDirect

Biochemical and Biophysical Research Communications

journal homepage: www.elsevier.com/locate/ybbrc

Development of a rapid culture method to induce adipocyte differentiation of human bone marrow-derived mesenchymal stem cells

Yuichi Ninomiya [a], Yzumi Sugahara-Yamashita [b], Yutaka Nakachi [b], Yoshimi Tokuzawa [b], Yasushi Okazaki [b], Masahiko Nishiyama [a,*]

[a] Translational Research Center, Saitama International Medical, Saitama Medical University, 1397-1 Yamane, Hidaka, Saitama 350-1298, Japan
[b] Division of Functional Genomics and Systems Medicine, Research Center for Genomic Medicine, Saitama Medical University, Saitama 350-1241, Japan

ARTICLE INFO

Article history:
Received 17 February 2010
Available online 3 March 2010

Keywords:
Mesenchymal stem cells
Adipocyte differentiation
Bone marrow
PPARγ

ABSTRACT

Human mesenchymal stem cells (hMSCs) derived from bone marrow are multipotent stem cells that can regenerate mesenchymal tissues such as adipose, bone or muscle. It is thought that hMSCs can be utilized as a cell resource for tissue engineering and as human models to study cell differentiation mechanisms, such as adipogenesis, osteoblastogenesis and so on. Since it takes 2–3 weeks for hMSCs to differentiate into adipocytes using conventional culture methods, the development of methods to induce faster differentiation into adipocytes is required. In this study we optimized the culture conditions for adipocyte induction to achieve a shorter cultivation time for the induction of adipocyte differentiation in bone marrow-derived hMSCs. Briefly, we used a cocktail of dexamethasone, insulin, methylisobutylxanthine (DIM) plus a peroxisome proliferator-activated receptor γ agonist, rosiglitazone (DIMRo) as a new adipogenic differentiation medium. We successfully shortened the period of cultivation to 7–8 days from 2–3 weeks. We also found that rosiglitazone alone was unable to induce adipocyte differentiation from hMSCs *in vitro*. However, rosiglitazone appears to enhance hMSC adipogenesis in the presence of other hormones and/or compounds, such as DIM. Furthermore, the inhibitory activity of TGF-β1 on adipogenesis could be investigated using DIMRo-treated hMSCs. We conclude that our rapid new culture method is very useful in measuring the effect of molecules that affect adipogenesis in hMSCs.

© 2010 Elsevier Inc. All rights reserved.

1. Introduction

Adipocytes store surplus dietary energy mainly as triglycerides [1,2]. In addition, adipocytes regulate glucose and lipid metabolism through the secretion of adipokines such as adiponectin and leptin [3–5]. Hypertrophy, an increase in the size of adipocytes, and hyperplasia, an increase in their number, cause obesity [6]. As obesity is associated with an increased risk of type II diabetes, hyperlipidemia and cardiovascular disease, it is one of the main public health problems, with the pathological condition referred to as 'metabolic syndrome'. The control of obesity is important for treating the deleterious condition of metabolic syndrome. So far, mouse cell lines (e.g. 3T3-L1, 3T3-F442A, ST2) or mouse embryonic fibroblasts (MEFs) have mainly been used as progenitor cells to study adipocyte differentiation and they have been useful for the elucidation of the molecular mechanism involved [7]. Using these cell lines, it was demonstrated that key regulators such as CCAAT/enhancer binding proteins (C/EBPs) and peroxisome proliferator-activated receptor γ (PPARγ) induce adipocyte differentiation [8–10]. In addition, they were used to show that transforming growth factor-β (TGF-β), Wnt, interleukin-1 (IL-1) and tumor necrosis factor-α (TNF-α) signaling suppress adipogenesis through the downstream transcription factors Smad2/3, β-catenin and NF-kB, respectively [11–15].

To understand human diseases and to explore possible cures for the associated diseases, it is important to study the molecular mechanism using human cells. A candidate for the adipocyte progenitor cells in humans is the mesenchymal stem cell (hMSC) derived from adult bone marrow. hMSCs contribute to the regeneration of mesenchymal tissues, such as adipose tissue, bone, cartilage or muscle [16]. It is thought that hMSCs can be utilized as a cell resource for tissue engineering and as human models to study cell differentiation such as adipogenesis and osteoblastogenesis [17]. Other than hMSCs, adipose tissue stromal cells have also been used to study adipogenesis, although it takes 2–3 weeks for these cells to differentiate into adipocytes [18,19]. The long period of time necessary for cells to differentiate into adipocytes from hMSCs has hampered the study of adipocyte differentiation using human cells (for example, in the search for adipogenesis inhibitory factors like TGF-β1 or inhibitory compounds).

In this study, we developed a new rapid culture method that induces differentiation of hMSCs into adipocytes efficiently in only

* Corresponding author. Fax: +81 42 984 4741.
E-mail address: yamacho@saitama-med.ac.jp (M. Nishiyama).

0006-291X/$ - see front matter © 2010 Elsevier Inc. All rights reserved.
doi:10.1016/j.bbrc.2010.03.001

7–8 days by optimizing the composition of the differentiation cocktail and the period of induction. The new culture method for hMSCs would serve as a good human cell model for research into adipocyte differentiation.

2. Materials and methods

2.1. Reagents

Rosiglitazone was purchased from Alexis Biochemicals (San Diego, CA), dexamethasone (DEX) was purchased from Wako (Tokyo, Japan), insulin was purchased from Invitrogen Corporation (Paisley, UK), methylisobutylxanthine (MIX) was purchased from Nacalai Tesque (Kyoto, Japan). TGF-β1 was purchased from R & D Systems (Minneapolis, MN). The anti-α/β-tubulin antibody was obtained from Cell Signaling (Boston, MA).

2.2. Cell culture and new protocol that rapidly induces to differentiate hMSCs into adipocytes

Human bone marrow-derived MSCs (hMSCs) were obtained from Cervex Bio Science Walkersville Inc. (Walkersville, MD). hMSCs were cultured in α-minimum essential medium (α-MEM) (Nacalai Tesque) supplemented with 10% heat-inactivated fetal bovine serum (FBS; Biological Industries, Ashrat, Israel) and penicillin (100 units/ml) and streptomycin (P/S) (100 μg/ml) (called normal medium). All incubation procedures were performed with 5% CO_2 in humidified air at 37 °C. For new rapid adipogenic induction on hMSCs, a-MEM supplemented with 10% FBS and P/S containing 250 nM DEX, 0.5 mM MIX, 5 μg/ml insulin (called DIMRo medium) plus 1 μM rosiglitazone was used. At first, postconfluent hMSCs were incubated with DIMRo medium for 3 days, moreover the culture medium was replaced with fresh DIMRo medium for 3 days, then the culture medium was replaced every 3 days with fresh normal medium. For the conventional adipogenic induction, the conventional differentiation medium (CDM), a-MEM supplemented with 10% FBS and P/S containing 1 μM DEX, 5 μg/ml insulin and 60 μM indomethacin was used. Briefly, postconfluent hMSCs were incubated with CDM for 3 days, then the culture medium was replaced every 3 days with fresh CDM.

2.3. Oil Red O staining

For Oil Red O staining, cells were fixed with 4% formaldehyde in PBS for 60 min and rinsed in PBS, water, and isopropanol sequentially. The cells were then stained with Oil Red O (0.3% in 60% isopropanol) for 20 min and rinsed three times with water.

2.4. RNA extraction and real-time quantitative RT-PCR (Q-PCR) analysis

Total RNA was isolated from hMSCs using Trizol reagent (Invitrogen). Q-PCR was performed as previously described [20]. In brief, total RNA was reverse-transcribed by Bioscript Reverse Transcriptase (Bioline, Luckenwalde, Germany) with oligo $(dT)_{18}$ primers. The reverse transcripts were used as templates for analysis of gene expression levels using Mx3000P (Stratagene; La Jolla, CA) and Power SYBR Green PCR Master Mix (Applied Biosystems; Warrington, UK) according to the manufacturer's instructions. RT-PCR analyses were performed using the following primers:

FABP4 (NM001442) Fwd, 5′-AACCTTAGATGGGGGTGTCC-3′;
FABP4 Rev, 5′-GTGGAAGTGACGCCTTTCAT-3′;
LPL (NM000237) Fwd, 5′-CTCTTGGGATACAGCCTTGG-3′;
LPL Rev, 5′-GGGGCTTCTGCATACTCAAA-3′;
PPARG (NM005037) Fwd, 5′-CCAGAAAGCGATTCCTTCAC-3′;
PPARG Rev, 5′-GAGAGATCCACGGAGCTGAT-3′;
GAPDH (NM002046) Fwd, 5′-ACACCCACTCCTCCACCTTT -3′;
GAPDH Rev, 5′-ATGAGGTCCACCACCCTGT-3′.

Data were normalized PPARG expression of non-treatment hMSCs using the DDC_T method as detailed in the manufacturer's guidelines of Applied Biosystems [20].

2.5. Western blot analysis

Nuclear extracts were prepared using the NE-PER nuclear and cytoplasmic extraction reagents (Thermo) according to the manufacture's protocol. Nuclear extract were subjected to Western blot as described [20]. The antibody for PPARγ [21] and the antibody for α/β-tubulin were used as primary antibodies. The horseradish peroxidase-conjugated mouse anti-rabbit IgG were used as secondary antibodies (Promega. Madison, WI). The blots were then incubated with the ECL plus reagents (Amersham Biosciences, Piscataway, NJ) and finally analyzed to LAS-1000 (Fujifilm, Tokyo, Japan).

3. Results

3.1. DIM plus rosiglitazone (DIMRo) treatment efficiently induces differentiation of bone marrow-derived hMSCs into adipocytes

DIM (a cocktail of dexamethasone, insulin, and methylisobutylxanthine) or rosiglitazone alone can induce adipogenesis of mouse 3T3-L1 cells [7,22,23]. Fajas et al. have shown that DIM plus rosiglitazone (DIMRo) induced more efficient adipocyte differentiation of MEFs compared with DIM [22]. As we would like to establish a culture method which induces differentiation of bone marrow-derived hMSCs into adipocytes in a shorter period of time, we examined the adipogenic effect of DIM, rosiglitazone alone or DIMRo using hMSCs. DIMRo-treated hMSCs accumulated lipid droplets in only 7–8 days (Fig. 1A) and in greater levels than DIM-treated cells (Fig. 1A). Interestingly, there were no Oil Red O-positive cells in hMSCs that were treated with rosiglitazone alone for 14–18 days, similar to the control cells (Fig. 1A). Corresponding with the results of the Oil Red O staining, DIMRo-treated hMSCs strongly expressed the adipogenic marker genes PPARG, fatty acid binding protein 4 (FABP4) and lipoprotein lipase (LPL), while DIM-treated hMSCs had modest expression compared with DIMRo-treated cells (Fig. 1B). As expected, rosiglitazone-treated hMSCs did not induce expression of these genes (Fig. 1B). Furthermore, to assess the effect of these adipogenic inducers on hMSCs, we elucidated the expression level of PPARγ proteins by Western blot analysis. DIMRo-treated cells strongly expressed both PPARγ1 and PPARγ2; DIM-treated cells had milder expression of both these proteins; while control and rosiglitazone-treated cells did not express these proteins (Fig. 1C). Taken together, DIMRo treatment efficiently induces differentiation of bone marrow-derived hMSCs into adipocytes displaying characteristics similar to differentiated MEFs.

3.2. DIMRo medium rapidly induces the accumulation of lipid droplets in bone marrow-derived hMSCs

To optimize the DIMRo medium cultivation conditions, we investigated the length of the DIMRo stimulation period required to induce adipocyte differentiation. After DIMRo treatment for 2, 4, 6 or 8 days, the medium was replaced with normal medium and lipid accumulation using Oil Red O staining assessed at day 8. A 6 day treatment with DIMRo most efficiently led to the accumulation of oil droplets (data not shown), so this stimulation time was used in further experiments.

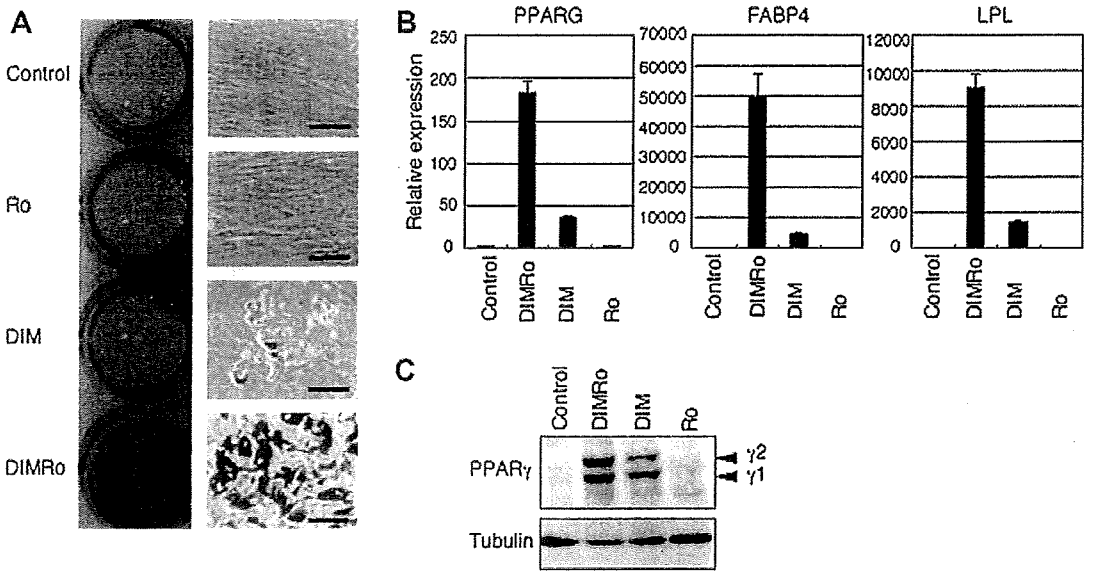

Fig. 1. The adipogenic effect of DIMRo, DIM and rosiglitazone on hMSCs. A, hMSCs were cultured with normal medium (control), rosiglitazone (1 μM), DIM or DIM plus rosiglitazone (DIMRo) for 6 days and were additively cultured with normal medium for 1 day. At day 7 after induction, hMSCs were stained by Oil Red O staining (left) and visualized by light microscopy (right). Scale bar, 100 μm. B, hMSCs were processed for Q-PCR analysis at day 7. The expression level of the adipogenic markers PPARG, FABP4 and LPL, was examined by Q-PCR. Error bars represent the means ± SD of triplicate determinations. Expression levels were normalized to GAPDH expression. C, Seven days after induction, nuclear extracts were prepared and subjected to Western blotting. The expression level of PPARγ protein was examined with anti-PPARγ and anti-α/β-tubulin antibodies. Each arrowhead represents the PPARγ1 and PPARγ2 isoform, respectively.

To assess the beneficial effect of this new method on the adipogenesis of hMSCs, we compared it with the traditional method using conventional differentiation medium (CDM, see materials and method). DIMRo-treated hMSCs accumulated lipid in only 7–8 days, while CDM-treated cells failed to do so (Fig. 2A and B). At 14 days after induction with CDM, a small number of cells began to accumulate oil droplets (Fig. 2B), while after 18 days, large numbers of CDM-treated cells became lipid-loaded cells, similar to DIMRo-treated cells (Fig. 2B). Taken together, DIMRo-treated hMSCs rapidly accumulate lipid droplets in a shorter period of time compared with CDM-treated cells.

3.3. DIMRo treatment rapidly induces expression of adipogenic marker genes in hMSCs

To determine whether DIMRo treatment induces expression of the adipogenic marker genes PPARG, FABP4 and LPL in hMSCs [24], we examined mRNA levels by Q-PCR. In DIMRo-treated hMSCs, expression of PPARG mRNA was strikingly increased at day 4, maintained at day 7 and decreased at day 14 (Fig. 3A). In CDM-treated hMSCs, expression of PPARG was only modestly induced at day 14, as was observed in DIMRo-treated cells (Fig. 3A). In DIMRo-treated cells, expression of FABP4 and LPL

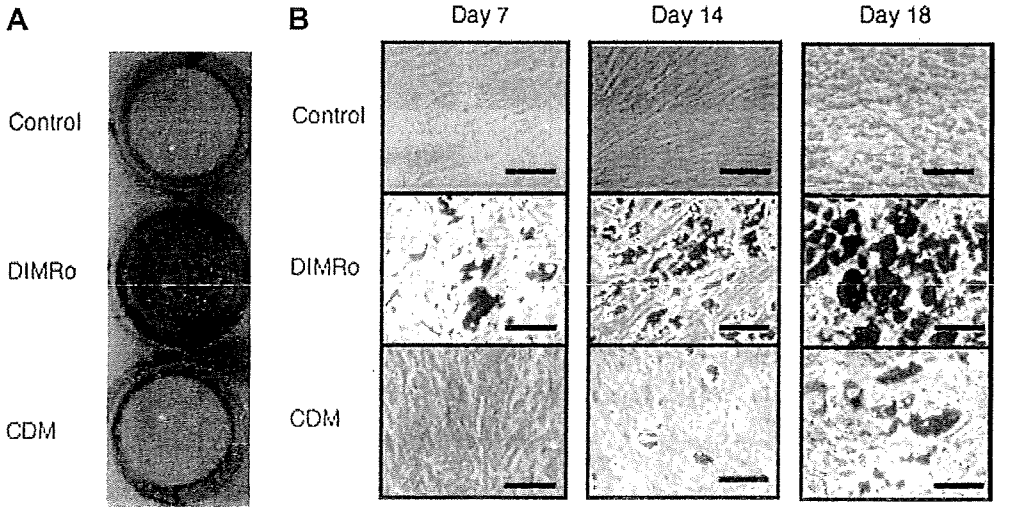

Fig. 2. The new culture method rapidly induces lipid accumulation in hMSCs. A, hMSCs were induced to differentiate using DIMRo medium or conventional adipogenic differentiation medium (CDM). DIMRo-treated cells were cultured with DIMRo medium for 6 days and then cultured with normal medium. CDC-treated cells were cultured continuously in CDC medium. Medium was changed every 3 days. After 7 days, hMSCs were examined by Oil Red O staining. B, At the indicated days, cells were stained by Oil Red O and visualized under the microscope. Scale bar, 100 μm.

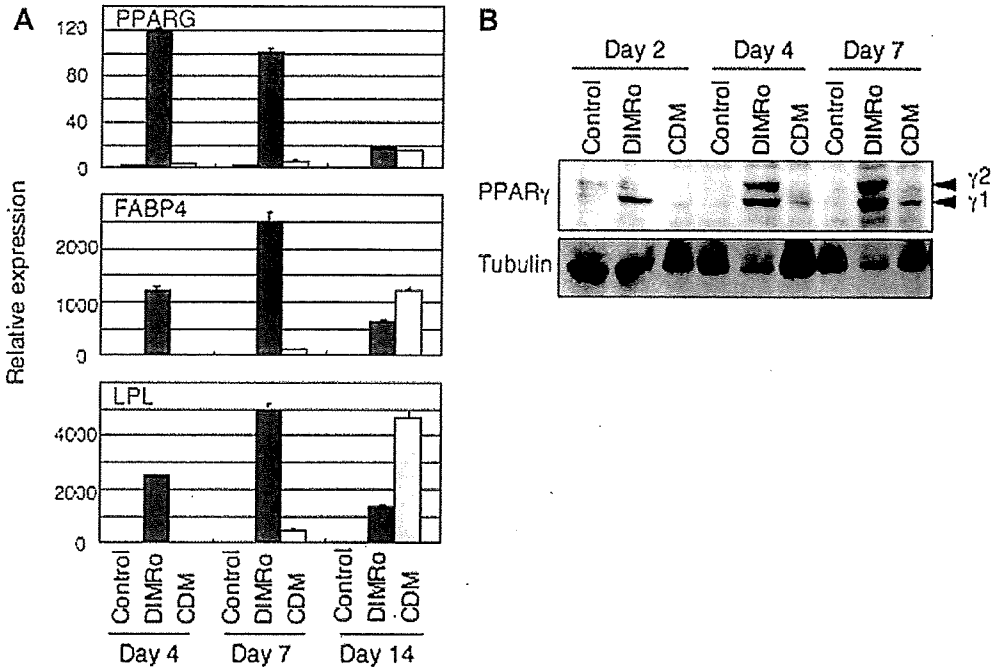

Fig. 3. DIMRo-treated hMSCs expressed adipogenic marker genes. A, hMSCs were cultured with normal medium, CDM or DIMRo medium and induced to differentiate into adipocytes. hMSCs were processed for Q-PCR analysis at days 4, 7 and 14. The expression level of the adipogenic markers PPARG, FABP4 and LPL was examined by Q-PCR as in Fig. 1B. Error bars represent the means ± SD of triplicate determinations. B, Expression of PPARγ proteins during adipocyte differentiation of hMSCs was examined by Western blotting as in Fig. 1C. Nuclear extracts were prepared and subjected to Western blot analysis. Each arrowhead represents PPARγ1 and PPARγ2 isoform, respectively.

mRNA was increased at day 4, increased further at day 7 and similar to PPARG, decreased at day 14 (Fig. 3A). In CDM-treated hMSCs, expression levels of FABP4 and LPL mRNA were very low at day 7 and increased at day 14 (Fig. 3A). We further analyzed the protein level of PPARγ, a key transcription factor of adipocyte differentiation by Western blotting. At day 2, DIMRo-treated but not control or CDM-treated cells expressed PPARγ1 (Fig. 3B). At days 4 and 7, DIMRo-treated cells also expressed PPARγ2 in addition to PPARγ1,

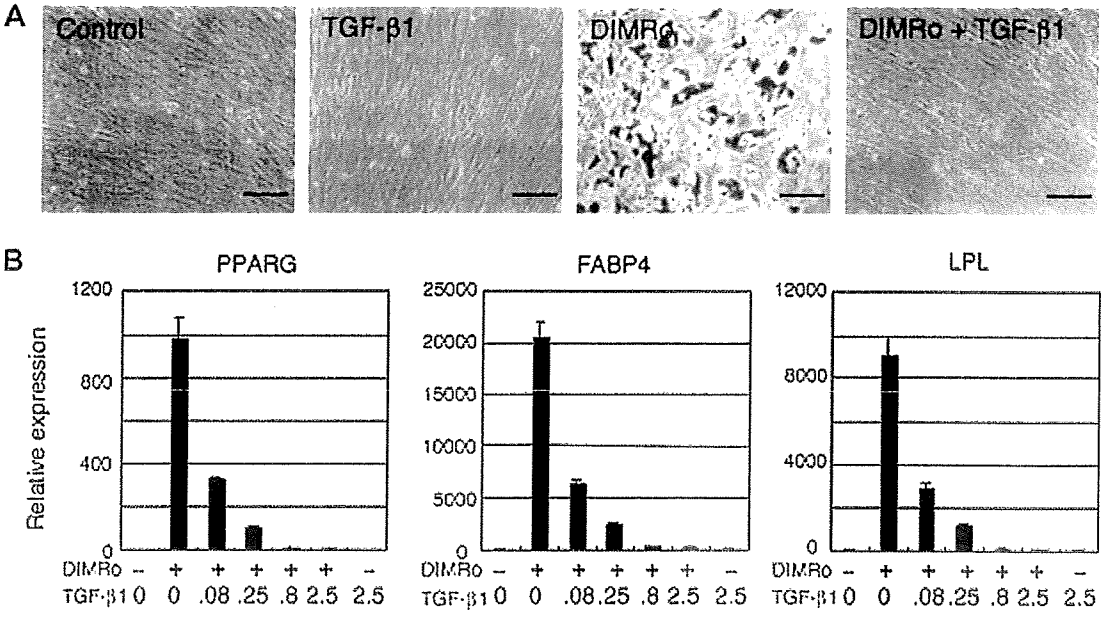

Fig. 4. DIMRo-treated hMSCs are sensitive to TGF-β1, an inhibitory factor of adipogenesis. A, hMSCs were cultured with normal medium (control), TGF-β1 (2.5 ng/ml), DIMRo or DIMRo plus TGF-β1 (2.5 ng/ml). At day 7, hMSCs were stained by Oil Red O staining and visualized under a light microscope. Scale bar, 100 μm. B, hMSCs were cultured with normal medium (control), TGF-β1 (2.5 ng/ml), DIMRo or DIMRo plus TGF-β1 at the indicated concentrations (ng/ml). At day 7, hMSCs were processed for Q-PCR analysis. The expression level of the adipogenic markers PPARG, FABP4 and LPL was examined by Q-PCR as in Fig. 1B. Error bars represent the means ± SD of triplicate determinations.

while CDM-treated cells only modestly expressed PPARγ1 but not PPARγ2 (Fig. 3B). Taken together, DIMRo treatment induces differentiation of hMSCs more rapidly into adipocytes compared with CDM-treated cells. The efficient induction of PPARγ2 proteins in DIMRo-treated cells dramatically enhances adipogenesis of hMSCs.

3.4. DIMRo-treated hMSCs are sensitive to TGF-β1, an inhibitory factor of adipogenesis

Since we wished to estimate the inhibitory effect of growth factors or cytokines (e.g. TGF-β and TNF-α) on the adipogenesis of hMSCs, we developed and optimized a new rapid culture method. DIMRo-treated hMSC cultures were treated with or without TGF-β1, an inhibitor of adipogenesis [11,12] and then examined using Oil Red O staining. TGF-β1 alone treated hMSCs did not accumulate lipid droplets, whereas DIMRo-treated hMSCs exhibited lipid accumulation in the absence of TGF-β1, a process that was inhibited by TGF-β1 (Fig. 4A). We further examined the expression of adipogenic marker genes by Q-PCR. Expression of adipogenic marker genes was markedly induced in DIMRo-treated hMSCs in the absence of TGF-β1 (Fig. 4B), but dose-dependently inhibited in the presence of TGF-β1 (Fig. 4B). These results demonstrate that DIMRo-treated hMSCs respond to inhibitory factor(s) of adipogenesis, such as TGF-β1.

4. Discussion

In this study, we have developed an efficient and rapid culture method for adipocyte differentiation of human bone marrow-derived MSCs. We have improved the culture conditions of the conventional method in two ways. First, we used DIMRo medium as an adipogenic induction cocktail. Second, we considered the optimal time period for induction of adipocyte differentiation of hMSCs by the adipogenic cocktail (data not shown). Consequently, the new culture method can accomplish adipocyte differentiation of hMSCs in only 7–8 days, compared with 2–3 weeks using the conventional method (Fig. 2). So far, although several studies have reported hMSC adipocyte differentiation using a similar adipogenic cocktail [16,18,19], the culture conditions were not adequately optimized.

In DIMRo-treated hMSCs, the mRNA expression of the adipogenic marker genes PPARG, FABP4 and LPL were expressed 4 days after induction and increased remarkably at day 7 (Fig. 3A). DIMRo-treated cells but not DIM- and CDM-treated cells expressed PPARγ2 protein at day 4 and 7 (Figs. 1C and 3B). Since DIMRo treatment significantly induces the expression of PPARγ2 protein in hMSCs, DIMRo appears to rapidly enhance adipocyte differentiation.

Thiazolidinediones (TZDs; e.g. rosiglitazone and pioglitazone) are agonists of PPARγ and are widely used in type II diabetes therapy. But over the past decade, animal studies have demonstrated that treatment of rodents with TZDs increased bone marrow adipocytes and consequently decreased bone formation and bone mass [24,25]. Recently, several clinical studies have also reported the adverse skeletal actions of TZDs in women [26,27]. Significantly, our data showed that rosiglitazone alone does not have a strong adipogenic activity on hMSCs because rosiglitazone-treated hMSCs did not accumulate lipid droplets even after 14 days or express adipogenic marker genes at day 7 (Fig. 1A and B). Rosiglitazone, however, did enhance the adipogenic effect of DIM (Fig. 1A and B). These results suggest that rosiglitazone induces adipogenesis of hMSCs by combining with other hormone(s) and/or compound(s). Using this new culture method, studying the mechanism of action of TZDs or other drugs will become more feasible. In addition, the new culture method can efficiently screen the effects of inhibitory factors of adipogenesis, such as TGF-β1 (Fig. 4).

Overall, the differentiation method developed here will save time and money for researchers investigating the adipogenesis of hMSCs. This method will also provide an efficient system for the screening of inhibitors or modifiers of adipocyte differentiation that might be candidates for drugs aimed at metabolic syndrome or patients with lipodystrophy.

Acknowledgments

We are grateful to Y. Yatsuka-Kanesaki and C. Shimizu for expert technical assistance. This work was supported by grants for the Genome Network Project from the Ministry of Education, Culture, Sports, Science and Technology (MEXT) of Japan to Y.O., and also in part by the Ministry of Education, Culture, Sports, Science and Technology (MEXT) of Japan, and in particular by a Ministry Grant to Saitama Medical University, Research Center for Genomic Medicine.

References

[1] E.D. Rosen, O.A. MacDougald, Adipocyte differentiation from the inside out, Nature Rev. Mol. Cell Biol. 7 (2006) 885–896.
[2] A. Guilherme, J.V. Virbasius, V. Puri, M.P. Czech, Adipocyte dysfunctions linking obesity to insulin resistance and type 2 diabetes, Nature Rev. Mol. Cell Biol. 9 (2008) 367–377.
[3] N. Rasouli, P.A. Kern, Adipocytokines and the metabolic complications of obesity, J. Clin. Endocrinol. Metab. 93 (2008) S64–S73.
[4] T. Kadowaki, T. Yamauchi, N. Kubota, K. Hara, K. Ueki, K. Tobe, Adiponectin and adiponectin receptors in insulin resistance, diabetes, and the metabolism, J. Clin. Invest. 116 (2007) 1784–1792.
[5] J.M. Friedman, J.L. Halaas, Leptin and the regulation of body weight in mammals, Nature 395 (1998) 763–770.
[6] M.D. Lane, Q.-Q. Tang, From multipotent stem cell to adipocyte, Birth Defects Res. 73 (2005) 476–477.
[7] A.K. Student, R.Y. Hsu, M.D. Lane, Induction of fatty acid synthetase synthesis in differentiating 3T3–L1 preadipocytes, J. Biol. Chem. 255 (1980) 4745–4750.
[8] O.A. MacDougald, P. Cornelius, F.-T. Lin, S.S. Chen, M.D. Lane, Glucocorticoids reciprocally regulate expression of the CCAAT/enhancer-binding protein α and δ genes in 3T3–L1 adipocytes and white adipose tissue, J. Biol. Chem. 269 (1994) 19041–19047.
[9] O.A. MacDougald, P. Cornelius, R. Liu, S.S. Chen, M.D. Lane, Insulin regulates transcription of the CCAAT/enhancer binding protein (C/EBP) α, β, and δ genes in fully-differentiated 3T3–L1 adipocytes, J. Biol. Chem. 270 (1995) 647–654.
[10] P. Tontonoz, E. Hu, R.A. Graves, A.I. Budavari, B.M. Spiegelman, MPPARγ2: tissue-specific regulator of an adipocyte enhancer, Genes & Dev. 8 (1994) 1224–1234.
[11] L. Choy, J. Skillington, R. Derynck, Roles of autocrine TGF-β receptor and Smad signaling in adipocyte differentiation, J. Cell Biol. 149 (2000) 667–681.
[12] L. Choy, R. Derynek, Transforming growth factor-β inhibits adipocyte differentiation by Smad3 interacting with CCAAT/enhancer-binding protein (C/EBP) and repressing C/EBP transcription function, J. Biol. Chem. 278 (2003) 9609–9619.
[13] S.E. Ross, N. Hemati, K.A. Longo, C.N. Bennett, P.C. Lucas, R.L. Erickson, O.A. MacDougald, Inhibition of adipogenesis by Wnt signaling, Science 289 (2000) 950–953.
[14] M. Suzawa, I. Takada, J. Yanagisawa, F. Ohtake, S. Ogawa, T. Yamauchi, T. Kadowaki, Y. Takeuchi, H. Shibuya, Y. Gotoh, K. Matsumoto, S. Kato, Cytokines suppress adipogenesis and PPAR-γ function through the TAK1/TAB1/NIK cascade, Nature Cell Biol. 5 (2003) 224–230.
[15] I. Takada, M. Mihara, M. Suzawa, F. Ohtake, S. Kobayashi, M. Igarashi, M.Y. Youn, K. Takeyama, T. Nakamura, Y. Mezaki, S. Takezawa, Y. Yogiashi, H. Kitagawa, G. Yamada, S. Takada, Y. Minami, H. Shibuya, K. Matsumoto, S. Kato, A histone lysine methyltransferase activated by non-canonical Wnt signalling suppresses PPAR-γ transactivation, Nat. Cell Biol. 9 (2007) 1273–1285.
[16] M.F. Pittenger, A.M. Mackay, S.C. Beck, R.K. Jaiswal, R. Douglas, J.D. Mosca, M.A. Moorman, D.W. Simonetti, S. Craig, D.R. Marshak, 1999 Multilineage potential of adult human mesenchymal stem cells, Science 284 (1999) 143–147.
[17] A.I. Caplan, Adult mesenchymal stem cells for tissue engineering versus regenetative medicine, J. Cell. Physiol. 213 (2007) 341–347.
[18] A.M. Rodriguez, C. Elabd, F. Delteil, J. Astier, C. Vernochet, P. Saint-Marc, J. Guesnet, A. Guezennec, E.Z. Amri, C. Dani, G. Ailhaud, 2004 Adipocyte differentiation of multipotent cells established from human adipose tissue, Biochem. Biophys. Res. Commun. 315 (2004) 255–263.
[19] W. Guo, J. Flanagan, R. Jasuja, J. Kirkland, L. Jiang, S. Bhasin, The effects of myostatin on adipogenic differentiation of human bone marrow-derived mesenchymal stem cells are mediated through cross-communication between Smad3 and Wnt/β-catenin signaling pathways, J. Biol. Chem. 283 (2008) 9136–9145.
[20] Y. Ninomiya, T. Yasuda, M. Kawamoto, O. Yuge, Y. Okazaki, Liver X receptor ligands inhibit the lipopolysaccharide-induced expression of microsomal

prostaglandin E synthase-1 and diminish prostaglandin E2 production in murine peritoneal macrophages, J. Steroid Biochem. Mol. Biol. 103 (2007) 44–50.
[21] Y. Nakachi, K. Yagi, I. Nikaido, H. Bono, M. Tonouchi, C. Schönbach, Y. Okazaki, Identification of novel PPARγ target genes by integrated analysis of ChIP-on-chip and microarray expression data during adipocyte differentiation, Biochem. Biophys. Res. Commun. 372 (2008) 362–366.
[22] L. Fajas, V. Egler, R. Reiter, J. Hansen, K. Kristiansen, M.-B. Debril, S. Miard, J. Auwerx, The Retinoblastoma-histone deacetylase 3 complex inhibits PPARγ and adipocyte differentiation, Dev. Cell 3 (2002) 903–910.
[23] M. Fu, T. Sun, A.L. Bookout, M. Downes, R.T. Yu, R.T. Yu, R.M. Evans, D.J. Mangelsdorf, A nuclear receptor atlas: 3T3–L1 adipogenesis, Mol. Endocrinol. 19 (2005) 2437–2450.
[24] S.O. Rzonca, L.J. Suva, D. Gaddy, D.C. Montague, B. Lecka-Czernik, Bone is a target for the antidiabetic compound rosiglitazone, Endocrinology 145 (2004) 401–406.
[25] A.A. Ali, R.S. Weinstein, S.A. Stewart, A.M. Parfitt, S.C. Manolagas, R.L. Jilka, Rosiglitazone causes bone loss in mice by suppressing osteoblast differentiation and bone formation, Endocrinology 146 (2005) 1226–1235.
[26] S.E. Kahn, S.M. Haffner, M.A. Heise, W.H. Herman, R.R. Holman, N.P. Jones, B.G. Kravitz, J.M. Lachin, M.C. O'Neill, B. Zinman, G. Viberti, A.D.O.P.T. Study Group, Glycemic durability of rosiglitazone, Metformin, or glyburide monotherapy. N. Engl. J. Med. 355 (2006) 2427–2443.
[27] A.V. Schwartz, D.E. Sellmeyer, E. Vittinghoff, L. Palermo, B. Lecka-Czernik, K.R. Feingold, E.S. Strotmeyer, H.E. Resnick, L. Carbone, B.A. Beamer, S.W. Park, N.E. Lane, T.B. Harris TB, S.R. Cummings, Thiazolidinedione use and bone loss in older diabetic adults, J. Clin. Endocrinol. Metab. 9 (2006) 3349–3354.

Carcinogenesis and cellular immortalization without persistent inactivation of p16/Rb pathway in lung cancer

MARINA ARIFIN[1], KEIJI TANIMOTO[1], ANDIKA CHANDRA PUTRA[1], EISO HIYAMA[2], MASAHIKO NISHIYAMA[1,3] and KEIKO HIYAMA[1]

[1]Department of Translational Cancer Research, Hiroshima University, Research Institute for Radiation Biology and Medicine (RIRBM); [2]Natural Science Center for Basic Research and Development, Hiroshima University, Hiroshima; [3]Translational Research Center, Saitama Medical University International Medical Center, Saitama, Japan

Received November 27, 2009; Accepted December 29, 2009

DOI: 10.3892/ijo_00000605

Abstract. Existence of cancer stem cells (CSCs) is still hypothetical and their practical marker is not available yet in lung cancer. To verify the possible existence of CSCs and to find their markers in lung cancer, we compared the p16/Rb and telomerase status in 83 lung cancer tissues and 15 lung cancer cell lines, since inactivation of p16/Rb pathway is considered to be a prerequisite for normal somatic cells to become immortal cancer cells. We found that 7 of 14 adenocarcinoma, but not squamous cell carcinoma, tissues with high telomerase activity and 3 adenocarcinoma cell lines likely had intact p16/Rb. Such cell lines showed higher colony formation capacity in soft agar compared with inactivated ones with similar growth rate. Moreover, cisplatin-resistant cell line PC9/CDDP with intact p16/Rb, but not PC14/CDDP with its inactivation, increased the colony formation capacity compared with the parent cells. Since CSCs are considered to be resistant to conventional anticancer drugs, they could have been concentrated as long as CSCs existed. We propose that half of immortal lung adenocarcinomas are derived from innately telomerase-positive stem cells, which might be the origin of CSCs, and that high telomerase activity with intact p16/Rb could be a marker of stem cell origin.

Introduction

The new concept describes a cancer stem cell (CSC) as a cell within a tumor that is able to self-renew and to produce the heterogenous lineages of cancer cells that comprise the tumor (1). Cancer stem cells have been speculated to be the source of many solid tumors including lung cancer (2), and be resistant to conventional chemo- and radio-therapy. Thus, identification of CSCs and their biomarkers in lung cancer is urgent to improve patient prognosis. Previously, CD133 (*PROM1*: prominin-1) positive cells (2,3), side population cells that extrude Hoechst 33342 dye (4), or aldehyde dehydrogenase positive cells (5) have been demonstrated to be the fractions of putative CSCs in malignant tumors including lung cancer, but they are still not conclusive (6).

It is widely accepted that CSCs have telomerase activity and are immortal so that they can produce cancer cells indefinitely (7-9). But it is not clear yet whether CSCs originate from normal stem cells or from differentiated somatic cells. Since human somatic cells are required to inactivate p16/Rb pathway to overcome cellular senescence and become immortal cancer cells concomitant with activation of telomerase (10,11), we hypothesized that immortal cancer cells without inactivation of p16/Rb pathway could not be derived from usual somatic cells, but be originated from innately telomerase-positive cells, i.e., stem cells. We previously found that all examined squamous cell carcinoma and small cell lung cancer (SCLC) tissues with high telomerase activity, meaning immortal cancer cells, had aberrations in *RB1* and/or *TP53* genes. However, in lung adenocarcinomas with high telomerase activity, neither gene was found in half of the samples (12). To verify this hypothesis, we examined p16 status in 83 lung cancer tissues and 15 lung cancer cell lines, and compared the relationship between the p16/Rb pathway status and the telomerase activity levels or colony formation capacities.

Materials and methods

Tumor samples. A total of 83 surgically resected primary lung cancer tissues, including 42 adenocarcinomas, 30 squamous cell carcinomas, 4 adenosquamous cell carcinomas, and 7 SCLCs, were obtained from chemotherapy-naïve patients, as well as the corresponding adjacent non-cancer lung tissue samples as controls. All tissues had been provided by the Department of Pathology and Department of Molecular and Internal Medicine, Hiroshima University between 1991-1996. Their pathological stages had been assessed according to the International Staging System (13) and telomerase activity, *RB1* loss of heterozygosity (LOH), *TP53* LOH, and chromo-

Correspondence to: Dr Keiko Hiyama, Department of Translational Cancer Research, Research Institute for Radiation Biology and Medicine, Hiroshima University, 1-2-3 Kasumi, Minami-ku, Hiroshima 734-8551, Japan
E-mail: khiyama@hiroshima-u.ac.jp

Key words: p16/Rb pathway, telomerase, cellular immortalization, cancer stem cells, lung cancer, adenocarcinoma

some 1p deletion mapping were previously reported (12,14-16). Written informed consent was obtained from all patients before surgery, and this study was approved by our Institutional Ethics Committee.

Cell lines. The SCLC cell line PC-6 and its SN-38- and CPT-11-resistant variants (SN2-5 and DQ2-2), a lung squamous cell carcinoma cell line LC-S, and lung adenocarcinoma cell lines PC-9 and PC-14 and their CDDP-resistant variants (PC-9/CDDP and PC-14/CDDP, respectively) as well as A549 were prepared and examined for CDDP sensitivity as previously described (17). The remaining 6 lung adenocarcinoma cell lines, RERF-LC-MS, VMRC-LCD, PC-3, RERF-LC-Ad1, RERF-LC-Ad2, and RERF-LC-KJ, and control fibroblast strain TIG-1 were obtained from the Health Science Research Resources Bank (Osaka, Japan).

Colony formation assay with soft agar. Anchorage-dependency of 11 lung adenocarcinoma cell lines was evaluated by conventional colony formation assay with soft agar in triplicate, as previous reported (18). Briefly, $5x10^3$ cells were cultured in 0.4% SeaPlaque GTG agarose (Bioproducts), and after 14 and 21 days of culture at 37°C with 5% CO_2, colony number was counted under microscopy for slow-growing cells (colonies containing >5 cells were counted) and macroscopically with crystal violet staining for rapid growing cells (colonies macroscopically visible were counted).

Preparation of DNA and RNA. For tissue samples, genomic DNA had been prepared previously (15). For cell lines genomic DNA and total RNA were extracted from the frozen cell pellets using QIAamp™ DNA Mini kit (Qiagen Inc., Valencia, CA) and Qiagen RNeasy™ mini kit (Qiagen), respectively, according to the manufacturer's protocols.

Real-time RT-PCR for evaluation of mRNA levels. For cell lines, 2 μg of total RNA was reverse-transcribed using High-Capacity cDNA Archive™ Kit (Applied Biosystems, Foster City, CA, USA). An aliquot of the cDNA (equivalent to 10 ng total RNA) was subjected to each real-time RT-PCR using Universal Probe Library (UPL, Roche Diagnostics, Tokyo, Japan) for *CDKN2A* (p16), *PROM1*, *BMI1*, and *ABCG2*, TaqMan Gene Expression Assays for *RB1* (Hs00153108_m1 targeting exons 24-25, Applied Biosystems), and Pre-Developed TaqMan Assay Reagents (Applied Biosystems) for ACTB as an internal control. Each reaction was carried out in duplicate or triplicate using ABI PRISM™ 7900HT Sequence Detection System (Applied Biosystems) and relative gene expression levels calculated as ratio to *ACTB* expression level were standardized using a pooled cDNA derived from 17 various cancer cell lines. The UPL primers (final concentration 200 nM each) and MGB-probe (final concentration 100 nM) sets are as follows: *CDKN2A*-F: 5'-GTGGACCTGGCTGAG GAG-3'. *CDKN2A*-R: 5'-CTTTCAATCGGGGATGTCTG-3'. *CDKN2A*-probe: UPL no. 34 (Roche). *PROM1*-F: 5'-AACCT TACACGAGCAAGGAATTA-3'. *PROM1*-R: 5'-AAACTTG TTCAAAAGTGAGCTTCAT-3'. *PROM1*-probe: UPL no. 48 (Roche). *BMI1*-F: 5'-TTCTTTGACCAGAACAGATTGG-3'. *BMI1*-R: 5'-GCATCACAGTCATTGCTGCT-3'. *BMI1*-probe: UPL no. 63 (Roche). *ABCG2*-F: 5'- TGGCTTAGACTCAAG CACAGC-3'. *ABCG2*-R: 5'-TCGTCCCTGCTTAGACA TCC-3'. *ABCG2*-probe: UPL no. 56 (Roche).

Real-time PCR for quantitation of DNA amounts. Homozygous deletion of *CDKN2A* was determined by TaqMan™ quantitative real-time PCR system with TagMan Universal PCR master mix and the ABI PRISM™ 7900HT Sequence Detection System (Applied Biosystems) using *TFRC* as control gene amount (12). Using a 384-well reaction plate (Applied Biosystems), 20 ng of genomic DNA and 2 sets of primers (final concentration 200 nM each for *CDKN2A* and 300 and 900 nM for *TFRC* forward and reverse primers, respectively) and fluorescent-probes (final concentration 100 nM for FAM-labeled *CDKN2A* and 200 nM for VIC-labeled *TFRC*) were mixed in a 10-μl reaction mixture. The primer and probe set for *TFRC* was previously reported (12) and that for *CDKN2A* is as follows: *CDKN2A*-F: 5'-AGCTTCCTTTCCGTCA TGC-3'. *CDKN2A*-R: 5'-TCATGACCTGCCAGAGAGAA-3'. *CDKN2A*-probe: UPL no. 21 (Roche). Threshold cycle (Ct) for each gene was determined using thermocycler software and the average of 3 independent Cts was calculated. Standard DNA was prepared by mixing genomic DNAs derived from two samples, non-cancer cells with intact *CDKN2A* and a cancer cell line with homologous deletion, at 10:0 (STD-100%), 8:2 (-80%), 6:4 (-60%), 4:6 (-40%), 2:8 (-20%), and 0:10 (0%).

Fragment analysis for detection of LOH. LOH of *CDKN2A* was evaluated by fragment length analysis using microsatellite marker D9S1748. The FAM-labeled forward primer (5'-CACCTCAGAAGTCAGTGAGT-3') and a non-labeled reverse primer (5'-GTGCTTGAAATACACCTTTCC-3') were mixed with 20 ng of genomic DNA and subjected to PCR followed by fragment analysis using ABI PRISM 310 Genetic Analyzer and GeneScan™ software as previously described (12). The adjacent non-cancer lung tissue samples were used as controls of peak height ratio of the corresponding repeat numbers.

Fragment analysis for quantitative methylation-specific PCR (qMSP). MSP was carried out to evaluate the *CDKN2A* (p16) CpG island methylation status according to a previous report (19) with quantitative modification. The bisulfite-treated genomic DNA was first amplified with outside non-fluorescent primers (35 cycles, annealing at 60°C) and then nested PCR was carried out using FAM-labeled methylated or HEX-labeled unmethylated allele-specific primers with annealing temperature at 65°C. Then, 0.5 μl each of methylated (FAM labeled) and unmethylated (HEX labeled) PCR products were mixed and subjected to ABI PRISM 310 Genetic Analyzer (Applied Biosystems). The methylation ratio was calculated as (area of FAM peak)/(areas of FAM peak + HEX peak).

Direct sequence analysis for RB1 cDNA. cDNAs derived from the 15 lung cancer cell lines were subjected to PCR using 2 sets of primers amplifying exons 10-26 that cover almost all naturally occurring *RB1* mutations. The PCR condition was 95°C for 15 min followed by 40 cycles of 95°C for 30 sec, 58°C for 1 min, and 72°C for 90 sec. Sequence analyses were carried out using Big Dye Terminator v1.1 Cycle Sequencing

Table I. The genetic aberrations in 83 primary lung cancers.

No.	Gender	Age	Stage	Tel[a]	*TP53*[a]	*RB1*[a]	1p34[a]	*CDKN2A* HD/LOH	*CDKN2A* qMSP	p16/Rb inactivation
Adenocarcinoma										
1	F	61	I	Low	Hetero	Hetero	Hetero	Hetero	1.0	+
2	M	69	I	Low	Hetero	Hetero	Hetero	Hetero	1.0	+
3	M	75	I	Low	Hetero	Hetero	Hetero	Hetero	1.0	+
4	M	62	I	Low	Hetero	Hetero	Hetero	Hetero	1.0	+
5	M	66	I	Low	Hetero	Hetero	Hetero	Hetero	1.0	+
6	F	67	I	Low	Hetero	Hetero	Hetero	Hetero	0.80	+
7	F	67	II	Low	Hetero	Hetero	Hetero	Hetero	1.0	+
8	M	76	IIIA	Low	Hetero	Hetero	Hetero	Hetero	0.99	+
9	M	61	IIIA	Low	Hetero	Hetero	Hetero	NI	1.0	+
10	M	60	IIIB	Low	Hetero	Hetero	Hetero	Hetero	0.27	+
11	F	64	IV	Low	Hetero	Hetero	Hetero	HD	0	+
12	F	56	IV	Low	Hetero	Hetero	Hetero	NI	0.59	+
13	F	57	IIIA	Low	Hetero	Hetero	LOH	NI	1.0	+
14	M	60	IV	Low	Hetero	Hetero	LOH	Hetero	1.0	+
15	F	65	IV	Low	Hetero	Hetero	LOH	LOH	0.88	+
16	F	62	I	Low	Hetero	LOH	LOH	Hetero	0.28	+
17	F	60	I	Low	NI	Hetero	Hetero	Hetero	0.90	+
18	M	48	I	Low	NI	Hetero	LOH	NI	1.0	+
19	F	51	IIIa	Low	NI	Hetero	Hetero	Hetero	1.0	+
20	F	57	I	Low	LOH	Hetero	LOH	LOH	0.69	+
21	M	58	IV	Low	LOH	Hetero	Hetero	Hetero	1.0	+
22	F	56	IV	Low	LOH	Hetero	Hetero	Hetero	1.0	+
23	M	66	IV	Low	LOH	Hetero	Hetero	Hetero	1.0	+
24	F	72	IIIA	Low	LOH	LOH	Hetero	Hetero	0.97	+
25	M	67	I	Low	LOH	LOH	LOH	Hetero	0.94	+
26	M	77	I	Low	LOH	LOH	LOH	NI	0.11	+
27	M	64	I	Low	LOH	LOH	LOH	Hetero	0.84	+
28	M	62	IIIA	Low	LOH	LOH	LOH	NI	0.10	+
29	F	78	I	High	Hetero	Hetero	Hetero	Hetero	0	-
30	M	69	I	High	Hetero	Hetero	Hetero	Hetero	0.87	+
31	M	62	I	High	Hetero	Hetero	Hetero	Hetero	0.11	-
32	M	75	I	High	Hetero	Hetero	Hetero	NI	0	-
33	F	62	II	High	Hetero	Hetero	Hetero	Hetero	0	-
34	F	69	IIIA	High	Hetero	Hetero	Hetero	Hetero	0.07	-
35	F	77	IV	High	Hetero	Hetero	Hetero	HD	0	+
36	F	80	I	High	Hetero	LOH	Hetero	Hetero	0	+
37	F	59	IIIA	High	LOH	Hetero	Hetero	Hetero	0.13	-
38	M	76	IIIA	High	LOH	Hetero	LOH	Hetero	0.15	-
39	M	55	I	High	LOH	LOH	LOH	HD	0	+
40	M	68	II	High	LOH	LOH	LOH	Hetero	0.10	+
41	M	66	IV	High	LOH	LOH	Hetero	Hetero	0.12	+
42	M	50	IIIB	High	LOH	LOH	LOH	Hetero	0	+
Adenosquamous cell carcinoma										
43	M	75	IIIA	Low	Hetero	Hetero	Hetero	HD	0	+
44	M	42	I	Low	NI	LOH	Hetero	NI	1.0	+
45	M	75	IV	Low	LOH	LOH	Amp	LOH	1.0	+
46	M	69	IIIA	High	LOH	LOH	LOH	HD	0.21	+

Table I. Continued.

No.	Gender	Age	Stage	Tel[a]	*TP53*[a]	*RB1*[a]	1p34[a]	*CDKN2A* HD/LOH	*CDKN2A* qMSP	p16/Rb inactivation
Small cell lung cancer										
47	M	75	I	Low	LOH	Hetero	LOH	Hetero	0	-
48	F	79	II	High	LOH	Hetero	Hetero	Hetero	0	-
49	M	56	I	High	LOH	LOH	Amp	Hetero	0	+
50	M	71	IIIA	High	LOH	LOH	Amp	Hetero	0.28	+
51	M	77	IIIA	High	LOH	LOH	Hetero	Hetero	0	+
52	M	74	I	High	LOH	LOH	LOH	HD	0	+
53	M	74	II	High	LOH	LOH	LOH	Hetero	0	+
Squamous cell carcinoma										
54	M	74	I	Low	Hetero	Hetero	Hetero	NI	0	-
55	F	62	I	Low	Hetero	Hetero	LOH	Hetero	0	-
56	M	70	II	Low	Hetero	Hetero	Hetero	NI	0	-
57	M	69	II	Low	Hetero	Hetero	Hetero	NI	0	-
58	M	63	II	Low	Hetero	Hetero	Hetero	Hetero	0	-
59	M	52	IIIA	Low	Hetero	Hetero	Hetero	Hetero	0	-
60	M	79	IIIA	Low	Hetero	Hetero	Hetero	Hetero	0	-
61	M	70	IIIA	Low	Hetero	Hetero	Hetero	LOH	0	+
62	M	69	IIIA	Low	Hetero	LOH	Hetero	LOH	0	+
63	M	77	IIIB	Low	Hetero	LOH	LOH	Hetero	0	+
64	M	61	II	Low	NI	Hetero	LOH	Hetero	0	-
65	M	72	I	Low	LOH	Hetero	Hetero	Hetero	NI	-
66	M	67	I	Low	LOH	Hetero	Hetero	LOH	0	+
67	M	60	IV	Low	LOH	Hetero	LOH	NI	0	-
68	M	71	I	Low	LOH	Hetero	LOH	HD	0	+
69	M	73	I	Low	LOH	LOH	Hetero	HD	0	+
70	M	87	I	Low	LOH	LOH	Hetero	Hetero	0	+
71	M	65	IIIA	Low	LOH	LOH	Hetero	LOH	0	+
72	F	71	I	Low	LOH	LOH	LOH	Hetero	0	+
73	M	63	I	Low	LOH	LOH	LOH	LOH	0	+
74	M	64	IIIA	Low	LOH	LOH	LOH	HD	NI	+
75	M	73	IV	Low	LOH	NI	Hetero	Hetero	0	-
76	M	66	I	Low	LOH	NI	LOH	Hetero	0	-
77	M	65	IIIA	Low	LOH	NI	LOH	LOH	0.02	-
78	M	72	IIIB	High	Hetero	LOH	LOH	LOH	0	+
79	M	62	IIIB	High	Hetero	LOH	LOH	Hetero	0	+
80	M	67	IIIA	High	LOH	Hetero	LOH	HD	0	+
81	M	62	IIIA	High	LOH	LOH	Hetero	HD	0	+
82	M	53	IV	High	LOH	LOH	LOH	NI	0	+
83	M	71	I	High	LOH	NI	LOH	HD	NI	+

[a]Previously analyzed for Tel (telomerase activity level), *TP53* (LOH in *TP53*), *RB1* (LOH in *RB1*), 1p34 (deletion within 1p34 to pter) (12,14-16). qMSP, (methylated allele peak)/(methylated + unmethylated allele peaks) area ratio >0.25 was considered as methylated; HD, homologous deletion; NI, not informative.

Kit™ and ABI PRISM 310 or PRISM 3100 Genetic Analyzer (Applied Biosystems). The 2 set primers are: *RB1*set1ex9-F: 5'-CTAATGGACTTCCAGAGGTTG-3'. *RB1*set1ex20-R: 5'-CGGAGATAGGCTAGCCGATA-3'. *RB1*set2ex19-F:

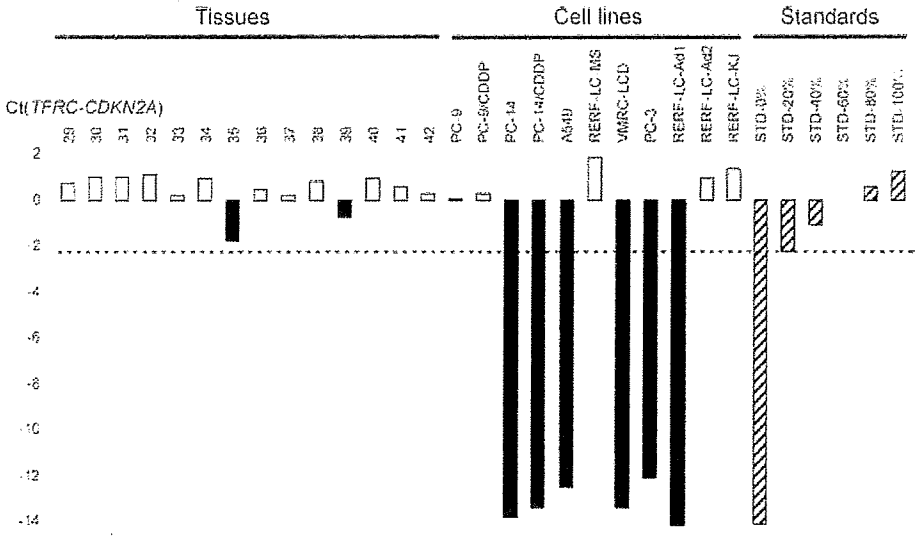

Figure 1. Detection of homologous deletion of p16 by quantitative real-time PCR for *CDKN2A* using control gene *TFRC* in representative samples (all adenocarcinoma tissues with high telomerase activity and lung adenocarcinoma cell lines). Tissue samples were classified as having homologous deletion when Ct(*TFRC*)-Ct(*CDKN2A*) in each sample < STD-60% (= 0, smooth line), and cell lines when < STD-20% (= -2.25, dotted line). Ct, threshold cycles; Hatched bar, standard DNA for quantitation; Closed bar, classified as homologous deletion; Open bar, classified as retaining at least one allele.

5'-TACTGCAAATGCAGAGACAC-3'. *RB1*set2ex27-R: 5'-GAAGAGGAAACAATCTGCTA-3'.

Telomerase activity and other genetic aberrations. Among the genetic aberrations in the tissue samples summarized in Table I, we previously evaluated and reported the telomerase activity level by TRAP assay (14), 1p34 LOH by deletion mapping using 12 polymorphic markers (16), and LOH of *TP53* and *RB1* genes using 5 and 4 polymorphic markers, respectively (12,15).

Statistical analysis. All statistical tests were performed using StatView version 5.0 software (SAS Institute Inc., Cary, NC, USA), and the Student's t-test, χ^2, or Fisher's exact test was used to determined the P-value. Differences of $P<0.05$ were considered statistically significant.

Results

Telomerase activity levels and LOH of *TP53*, *RB1*, and 1p34 locus in the lung cancer tissues have been evaluated previously (12,14-16) and summarized in Table I with the present data.

p16 inactivation. Persistent type inactivation of p16 was evaluated by the existence of *CDKN2A* homozygous deletion, LOH, and/or promoter methylation in 83 lung cancer tissues, and by *CDKN2A* homozygous deletion or complete promoter methylation in 15 lung cancer cell lines.

Homozygous deletion, [threshold cycles (Ct) of *TFRC*]-(Ct of *CDKN2A*) was smaller in a sample than that of 60% (for tissue samples) or 20% (for cell lines) standards in real-time PCR considering the existence of contaminated non-cancer cells in tissue samples, was found in 3 adenocarcinoma, 6 squamous cell carcinoma, 2 adenosquamous cell carcinoma, and 1 SCLC tissues and 6 adenocarcinoma cell lines (Fig. 1) and 1 squamous cell carcinoma cell line, LC-S. LOH, i.e., the calculated peak height ratio of the 2 alleles was <70% or >150% of that in normal counterpart in fragment analysis, was found in 10 tissue samples (Fig. 2). Cell lines could not be analyzed for LOH due to the lack of normal counterpart.

For evaluating *CDKN2A* promoter methylation, we considered it methylated when the methylated allele ratio, (methylated allele peak area)/(methylated and unmethylated allele peak areas), was >25%, and complete methylation when the ratio was >80% (Fig. 3). The *CDKN2A* promoter methylation was detected in 61.9% (26/42) of adenocarcinoma, but none of squamous cell carcinomas. For lung cancer cell lines, RERF-LC-MS was completely methylated among the 8 cell lines that retained *CDKN2A* gene. Thus, p16 inactivation by deletion or promoter methylation is summarized in Tables II and III, and such inactivation in adenocarcinoma tissues revealed to be highly associated with low/nil telomerase activity (P=0.0001).

Rb inactivation. Inactivation of Rb was evaluated by the existence of *RB1* LOH (analyzed for 1 RFLP and 3 microsatellite loci) in 83 lung cancer tissues and by the existence of genetic aberrations in *RB1* cDNA (sequence analysis of exons 10-27, that cover the mutation hot-spot region) or absence of *RB1* mRNA detection (real-time RT-PCR) in the 15 lung cancer cell lines.

For the 83 lung cancer tissue samples, we previously analyzed and reported that *RB1* LOH was found in 26 (34.2%) of 76 non-small cell lung cancer (NSCLC) and 5 (71.4%) of 7 SCLC tissues (12,15). Among the 15 lung cancer cell lines examined, *RB1* expression could not be detected in 1 adenocarcinoma cell line, RERF-LC-KJ (Fig. 4A). Also by sequence analysis of *RB1* cDNA, only this cell line was revealed to have an aberration, an inframe deletion of 174 nucleotides by splicing out the entire exons 24 and 25.

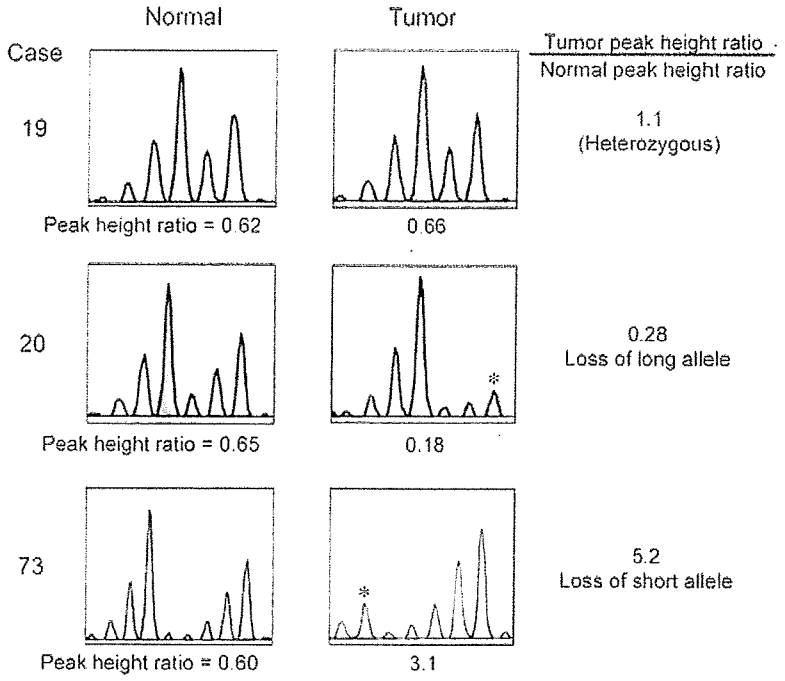

Figure 2. Detection of LOH of p16 by fragment analysis in representative samples. LOH, in cancer tissues was defined when the peak height ratio of heterozygous bands was <0.7 or >1.5 of expected ratio calculated from the normal counterpart. *Deleted allele demonstrating low peak possibly derived from contaminated non-cancer cells.

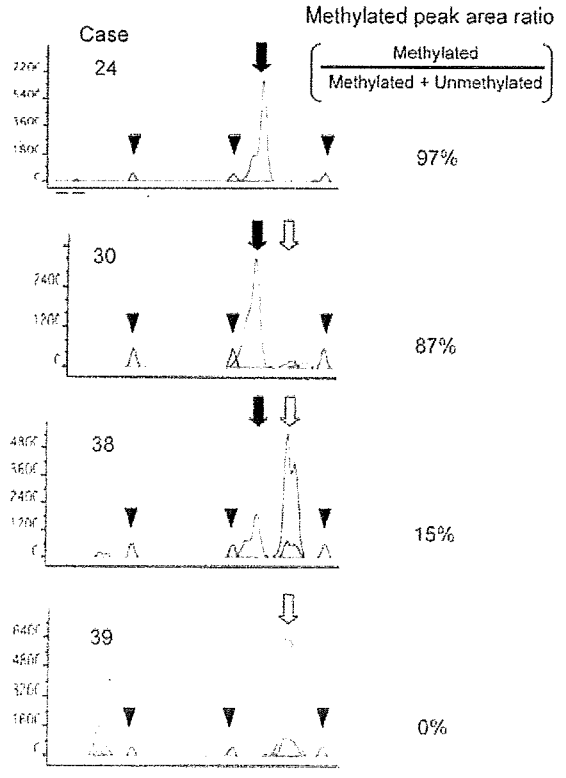

Figure 3. Quantitative evaluation of promoter methylation of p16 by fragment analysis in representative adenocarcinoma tissues. Methylated allele was labeled with FAM (closed arrow) and unmethylated allele was labeled with HEX (open arrow). The methylation ratio was calculated as (area of FAM peak)/(sum of areas of FAM & HEX peaks), and >25% was considered to be methylated and >80% as completely methylated. Arrowhead, size marker.

Inactivation of p16/Rb pathway. Combining above, inactivation of p16/Rb pathway, i.e., deletion/methylation of p16 and/or LOH of *RB1*, among the 83 lung cancer tissues was found in all 28 (100%) with low/nil telomerase activity but in only 7 of 14 (50%) with high telomerase activity (P=0.0001) in adenocarcinomas, whereas this relationship was the opposite in the remaining histology tumors (P=0.0309) (Table II). The p16 inactivation was inversely correlated with *RB1* LOH in adenocarcinoma tissues (P=0.0488).

Among the 15 lung cancer cell lines, the Rb inactivated cell line RERF-LC-KJ showed intact p16 as expected. Among the 11 adenocarcinoma cell lines, the p16/Rb pathway was considered to be intact in PC-9, its CDDP resistant variant PC-9/CDDP, and RERF-LC-Ad2 (p16/Rb pathway intact group) and inactivated in the remaining 8 cell lines (inactivated group). Then, cellular growth rate and colony formation capacity were carried out between these 2 groups.

Expression of cancer stem cell markers. As known cancer stem cell markers, we evaluated mRNA expression levels of *PROM1* (CD133), *BMI1*, and *ABCG2* by real-time RT-PCR in the 15 lung cancer cell lines. While the expression levels of *BMI1* and *ABCG2* genes were comparable among the all cell lines except for *ABCG2* in the drug resistant SCLC clones, *PROM1* was highly expressed in RERF-LC-Ad2, in which the p16/Rb pathway was considered to be intact (Fig. 4B).

Growth rate of adenocarcinoma cell lines. We found that the 11 adenocarcinoma cell lines can be divided into 2 groups according to their growth rates: >20 times multiplied at day 5 (rapid growth group, Fig. 5A) and less than that (slow growth group, Fig. 5B). The p16/Rb-intact cell lines PC-9 and PC-9/

Table II. Inactivation of p16/Rb in 83 lung cancer tissues.

Histology	Telomerase activity[a]	*RB1* LOH[a]	p16 inactivation	p16 and/or Rb inactivation
Adenocarcinoma				
	High (n=14)	5 (35.7%)	3 (21.4%)	7 (50%)
	Low/nil (n=28)	6 (21.4%)	26 (92.9%)	28 (100%)
Adenosquamous cell carcinoma				
	High (n=1)	1 (100%)	1 (100%)	1 (100%)
	Low/nil (n=3)	2 (66.7%)	3 (100%)	3 (100%)
Squamous cell carcinoma				
	High (n=6)	4 (66.7%)	4 (66.7%)	6 (100%)
	Low/nil (n=24)	8 (33.3%)	9 (37.5%)	12 (50.0%)
Small cell lung cancer				
	High (n=6)	5 (83.3%)	2 (33.3%)	5 (83.3%)
	Low/nil (n=1)	0 (0%)	0 (0%)	0 (0%)

[a]Previously analyzed for telomerase activity level and *RB1* LOH (12,14-16).

Table III. Inactivation of p16/Rb in lung cancer cell lines.

	Rb inactivation		p16 inactivation		
Histology	RT-PCR[a]	Deletion	HD	qMSP	p16/Rb inactivation
Adenocarcinoma					
PC-9	-	-	-	0.46	-
PC-9/CDDP	-	-	-	0.40	-
PC-14	-	-	+	NI	+
PC-14/CDDP	-	-	+	NI	+
A549	-	-	+	NI	+
RERF-LC-MS	-	-	-	1.0	+
VMRC-LCD	-	-	+	NI	+
PC-3	-	-	+	NI	+
RERF-LC-Ad1	-	-	+	NI	+
RERF-LC-Ad2	-	-	-	0	-
RERF-LC-KJ	+	+	-	0	+
Squamous cell carcinoma					
LC-S	-	-	+	NI	+
Small cell lung cancer					
PC-6	-	-	-	0.01	-
SN2-5	-	-	-	0.04	-
DQ2-2	-	-	-	0.16	-

[a]RT-PCR +, not detectable by real-time RT-PCR; qMSP. methylation ratio >0.8 was considered as completely inactivated; HD, homologous deletion; NI, not informative.

CDDP in the former group and RERF-LC-Ad2 in the latter group did not show accelerated growth compared to the inactivated ones in each group.

Colony formation assay with soft agar. While the colonies in the rapid growth group were evaluated macroscopically after crystal violet staining (Figs. 5C and 6), those in the slow

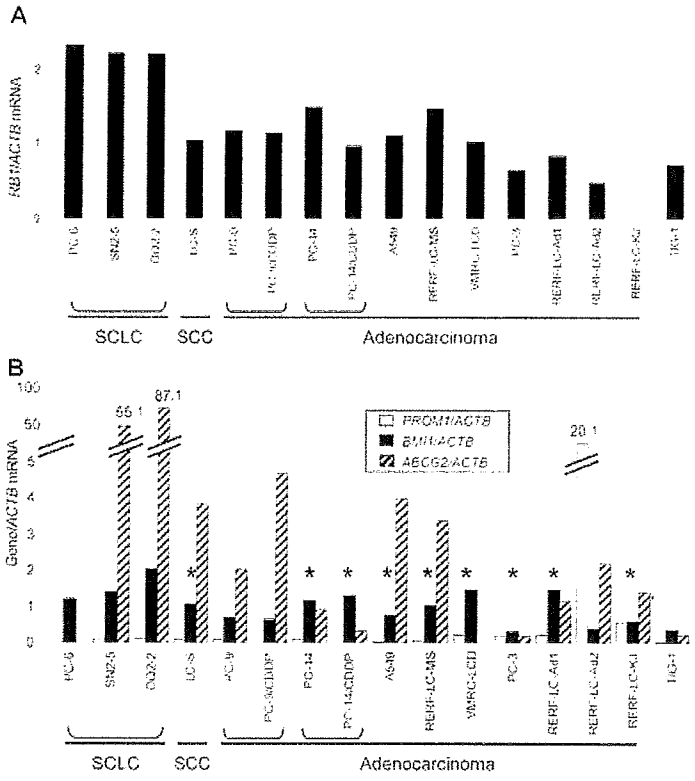

Figure 4. mRNA expression levels in all 15 cell lines evaluated by real-time RT-PCR using *ACTB* as internal control. *RB1* was not detected in RERF-LC-KJ (A). *PROM1* (open bar) was highly expressed in RERF-LC-Ad2, while the expression levels of *BMI1* (closed bar) and *ABCG2* (hatched bar) genes were comparable except for the drug resistant SCLC clones for *ABCG2* (B). Cell lines inactivated for p16/Rb pathway (homologous deletion or complete methylation of p16 or complete inactivation of *RB1*) are indicated by asterisk. TIG-1 is a non-cancer control human fibroblasts.

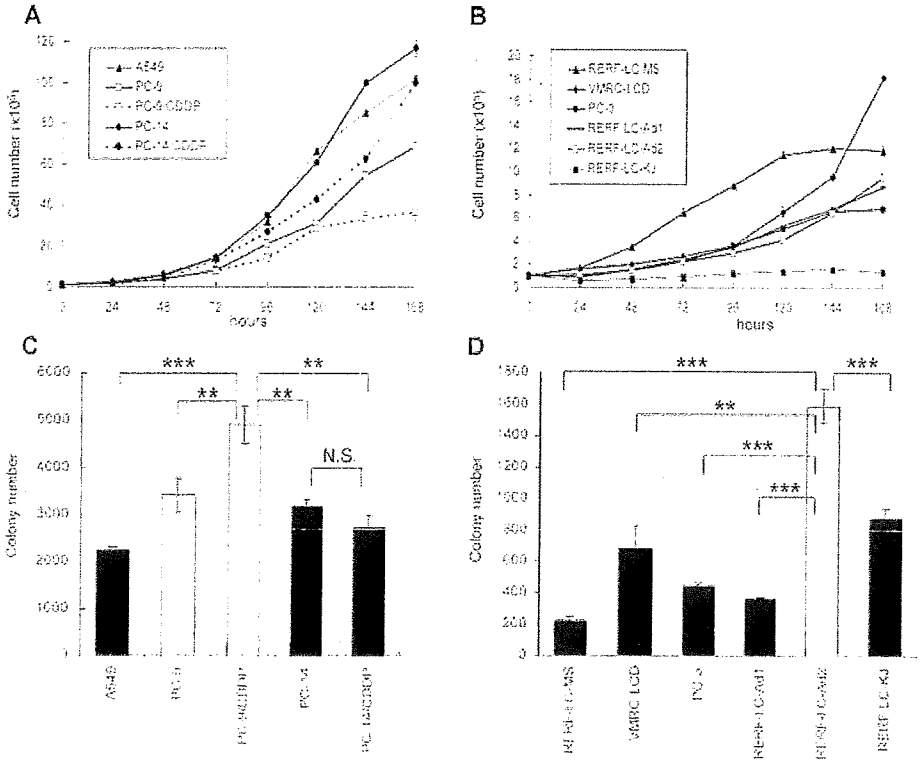

Figure 5. Growth rate and colony numbers in colony formation assay for the 11 lung adenocarcinoma cell lines. In each 60-mm diameter dish, 10^5 each of rapid growth cell lines (A) or slow growth cell lines (B) were cultured, and cell number was calculated every day for 1 week in triplicate. Colony numbers of the rapid growth cell lines were evaluated macroscopically after crystal violet staining (C) while those of the slow growth cell lines were evaluated microscopically (D). p16/Rb intact cell lines (open box) did not show higher growth but showed increased colonies (open bar) in soft agar compared to p16/Rb inactivated cell lines (closed bar) in each group. $^{**}P<0.01$; $^{***}P<0.001$; N.S., not significant.

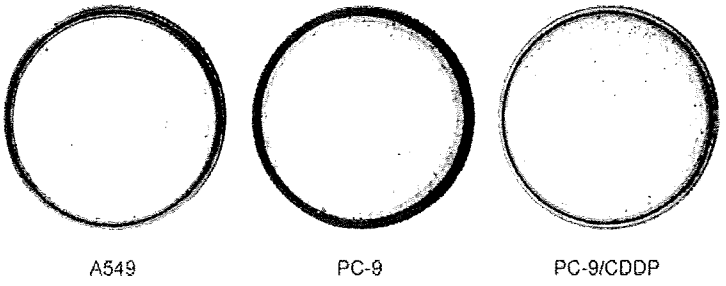

Figure 6. Colony formation assay for representative adenocarcinoma cell lines with rapid growth. Macroscopically visible colonies shown after crystal violet staining are p16/Rb inactivated cell line A549 < p16/Rb intact PC-9 < CDDP resistant PC-9 variant PC-9/CDDP.

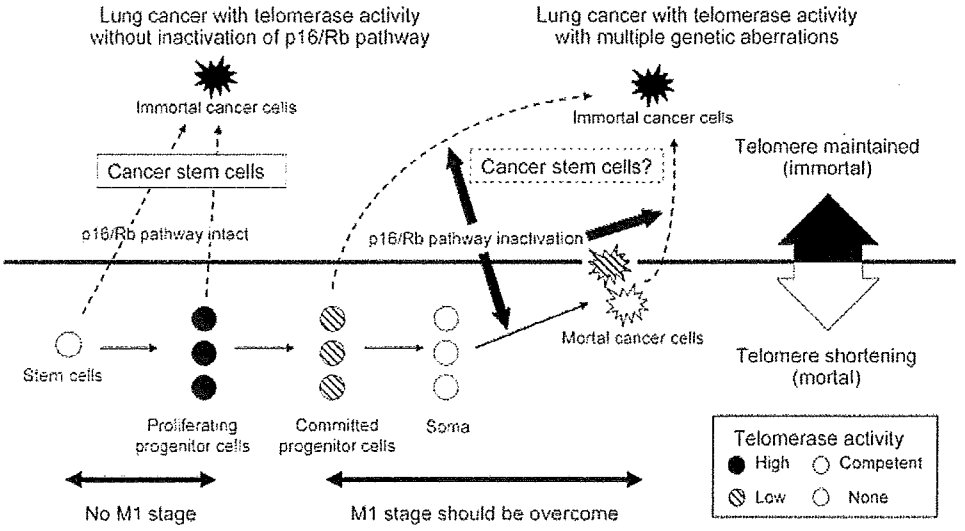

Figure 7. Our hypothesis of lung carcinogenesis. Immortal lung cancer cells might be derived from either of the two pathways: developed from telomerase positive normal cells, i.e., stem cells, through cancer stem cells or from telomerase negative somatic cells through multiple clonal selections acquiring genetic aberrations including *TP53*, *CDKN2A*, and *RB1* inactivations and telomerase activation, but not necessarily through cancer stem cells. Half of lung adenocarcinomas with high telomerase activity may develop from the former pathway, while most of squamous cell carcinomas develop from the latter pathway. M1, mortality stage 1; M2, mortality stage 2.

growth group were evaluated microscopically before staining, since they were small and macroscopically invisible in general even after 3 weeks (Fig. 5D). The p16/Rb intact cell lines, PC-9 and PC-9/CDDP in the rapid growth group and RERF-LC-Ad2 in the slow growth group, showed significantly higher colony formation capacity than the p16/Rb inactivated cell lines in each group (P<0.01-P<0.0001). Moreover, CDDP-resistant clone with intact p16/Rb (PC-9/CDDP), but not that with p16/Rb inactivation (PC-14/CDDP), showed significantly higher colony formation capacity than the parent clone (P<0.001, Figs. 5C and 6).

Discussion

Most malignant tumors must have a mechanism for bypassing senescence to acquire the unlimited proliferative capacity that is required for advanced cancers. Human somatic cells are considered to have two stages of checkpoint before acquiring immortality (two-stage model for cellular senescence): mortality stage 1 (M1) that can be overcome by inactivation of p16/Rb and p53 pathways and mortality stage 2 (M2), that requires activation of telomerase to be overcome (11,20). In fact, we previously found that all examined lung squamous cell carcinoma and SCLC tissues with high telomerase activity had aberrations in *RB1* and/or *TP53* genes. However, in lung adenocarcinomas with high telomerase activity, neither gene was found in half of them (12). We also showed that cancer tissues with high telomerase activity consisted of predominantly telomerase positive cells, i.e., immortal cancer cells, while those with low telomerase activity consisted of predominantly telomerase negative cells (21), and lung cancer cell lines always showed high telomerase activity (14). In addition, we confirmed full-length type *TERT* mRNA expression in all 15 lung cancer cell lines used in the present study by real-time RT-PCR, which had been confirmed to correlate with telomerase activity (22). Since we previously found that lung cancers which might have originated from telomerase positive bronchial epithelia always showed high telomerase activity (23), lung cancers with high telomerase activity, consist of predominantly immortal cancer cells, and immortal lung cancer cell lines might have been derived from either of the two pathways:

developed from telomerase positive normal cells, i.e., stem cells, or from telomerase negative somatic cells through multiple clonal selections acquiring genetic aberrations including *TP53*, *CDKN2A*, and/or *RB1* inactivation and telomerase activation.

To confirm this hypothesis, we examined incidence of persistent type p16 inactivation (deletion and/or methylation of *CDKN2A*) in the tissue samples as well as p16/Rb status and colony formation capacity in cell lines in the present study. It has been reported that the inactivation of p16 occurs most prominently through promoter methylation or homozygous deletion and less often through mutation in lung cancers (24). As we speculated, persistent inactivation of p16/Rb pathway, deletion of *CDKN2A* or *RB1* or methylation of *CDKN2A* promoter, was found in all adenocarcinoma tissues with low/nil telomerase activity, while neither was found in half of adenocarcinomas with high telomerase activity (P=0.0001). For other genetic aberrations, we previously reported that the *RB1* LOH was associated with *TP53* and 1p34 LOH but not with *EGFR* aberrations (12). In the present study, 5 of 7 p16/Rb intact adenocarcinomas with high telomerase activity also lacked the *TP53* LOH and 4 of them lacked both *TP53* and 1p34 LOH (Table I), indicating that these cases have escaped the M1 stage without persistent inactivation of p16/Rb pathway, p53 pathway, and the unknown pathway involving 1p34 locus. The importance of the p16/Rb and p53 pathways in lung epithelial cells is known by the high incidence of their defects in any histological type of lung cancer (25), and the adenocarcinomas without their persistent inactivation may have come without these checkpoints.

It has been indicated that only a small proportion of the tumor cells are able to form colonies in an *in vitro* colonogenic assay (26), and we found that adenocarcinoma cell lines without persistent inactivation of p16/Rb pathway had higher colony formation capacity in soft agar. Moreover, CDDP-resistant clone with intact p16/Rb (PC-9/CDDP), but not one with inactivation (PC-14/CDDP), showed higher colony formation capacity than the parent clones. Although the evidence is not sufficient yet, this could be explained that the former contained CSCs and enriched them in the CDDP-resistant clone, because CSCs are considered to be resistant to conventional chemotherapeutic drugs (2), while the latter did not contain CSCs originally and could not enrich the resistant clone. We also examined the expression levels of the known cancer stem cell markers, *PROM1* (2), *BMI1* (7), and *ABCG2* (27) in 15 lung cancer cell lines, and found that the p16/Rb intact cell line RERF-LC-Ad2 showed markedly high expression of *PROM1*, supporting our hypothesis that the p16/Rb intact immortal cancer cells may have derived from stem cells, and none of the presently available CSC markers is sufficient for all types of lung cancer.

Taken together, the present data indicate that 7 (50%) of 14 lung adenocarcinoma tissues with high telomerase activity (indicating they are predominantly consist of immortal cancer cells) and 3 of 11 (or 2 of 9 parent) lung adenocarcinoma cell lines, PC-9, PC-9/CDDP, and RERF-LC-Ad2, may have developed from M1 escaped cells, i.e., innately telomerase-positive stem cells, which are considered to be the origin of CSCs. Some of SCLC may have derived from such cells, because 1 of 6 SCLC tissues with high telomerase activity and 1 original (PC-6) as well as its 2 drug-resistant cell clones showed intact p16/Rb pathway (Fig. 7). However, for squamous cell carcinoma, no tissue with high telomerase activity nor the cell line examined showed intact p16/Rb pathway, indicating that it is always required to overcome the M1 stage to become immortal squamous cell carcinoma cells and that the telomerase-negative somatic cells may be of such origin. This speculation may be partly supported by the facts that squamous cell carcinoma often demonstrates evidence of multistep carcinogenesis, i.e., hyperplasia, metaplasia, dysplasia, carcinoma *in situ*, and invasive cancer, while adenocarcinoma and SCLC often lack such precancerous lesions indicating *de novo* carcinogenesis. Thus, we propose that there are two distinct pathways in lung carcinogenesis: one from primarily telomerase-positive cells, i.e., stem cells, independent of p16/Rb checkpoint mechanism in M1 stage, while the other from telomerase-negative somatic cells overcoming the M1 stage by inactivation of the p16/Rb and p53 pathways.

In conclusion, our study showed new important insights into lung CSCs. In particular, high telomerase expression without p16/Rb aberration possibly is a marker of cancer stem cells in lung cancers. Although further experiments are necessary to confirm our hypothesis, it could be an important key to study the molecular mechanisms of lung carcinogenesis and clinical implications.

Acknowledgments

We are grateful to Professor K. Inai at the Department of Pathology and Professor N. Kohno at the Department of Molecular and Internal Medicine, Hiroshima University, for providing sample tissues. We also thank Ms. I. Fukuba, Ms. M. Wada, Ms. C. Oda, and Ms. H. Tagawa in our departments for their technical support. Part of this work was carried out at the Department of Molecular and Internal Medicine and the Analysis Center of Life Science, Hiroshima University. This study was partly supported by Grants-in-Aid for Scientific Research from the Ministry of Education, Culture, Science, Sports and Technology of Japan.

References

1. Clarke MF, Dick JE, Dirks PB, Eaves CJ, Jamieson CH, Jones DL, Visvader J, Weissman IL and Wahl GM: Cancer stem cells - perspectives on current status and future directions: AACR Workshop on cancer stem cells. Cancer Res 66: 9339-9344, 2006.
2. Eramo A, Lotti F, Sette G, Pilozzi E, Biffoni M, Di Virgilio A, Conticello C, Ruco L, Peschle C and De Maria R: Identification and expansion of the tumorigenic lung cancer stem cell population. Cell Death Differ 15: 504-514, 2008.
3. Mizrak D, Brittan M and Alison MR: CD133: molecule of the moment. J Pathol 214: 3-9, 2008.
4. Hirschmann-Jax C, Foster AE, Wulf GG, Nuchtern JG, Jax TW, Gobel U, Goodell MA and Brenner MK: A distinct 'side population' of cells with high drug efflux capacity in human tumor cells. Proc Natl Acad Sci USA 101: 14228-14233, 2004.
5. Jiang F, Qiu Q, Khanna A, Todd NW, Deepak J, Xing L, Wang H, Liu Z, Su Y, Stass SA and Katz RL: Aldehyde dehydrogenase 1 is a tumor stem cell-associated marker in lung cancer. Mol Cancer Res 7: 330-338, 2009.
6. Meng X, Li M, Wang X, Wang Y and Ma D: Both CD133$^+$ and CD133$^-$ subpopulations of A549 and H446 cells contain cancer-initiating cells. Cancer Sci 100: 1040-1046, 2009.

7. Lobo NA, Shimono Y, Qian D and Clarke MF: The biology of cancer stem cells. Annu Rev Cell Dev Biol 23: 675-699, 2007.
8. Hiyama E and Hiyama K: Telomere and telomerase in stem cells. Br J Cancer 96: 1020-1024, 2007.
9. Hiyama K, Hiyama E, Tanimoto K and Nishiyama M: Role of telomeres and telomerase in cancer. In: Telomeres and Telomerase in Cancer. Hiyama K (ed.). Humana Press, Springer, New York, NY, pp171-180, 2009.
10. Shapiro GI, Edwards CD, Ewen ME and Rollins BJ: $p16^{INK4A}$ participates in a G1 arrest checkpoint in response to DNA damage. Mol Cell Biol 18: 378-387, 1998.
11. Shay JW and Wright WE: Senescence and immortalization: role of telomeres and telomerase. Carcinogenesis 26: 867-874, 2005.
12. Arifin M, Hiyama K, Tanimoto K, Wiyono WH, Hiyama E and Nishiyama M: EGFR activating aberration occurs independently of other genetic aberrations or telomerase activation in adenocarcinoma of the lung. Oncol Rep 17: 1405-1411, 2007.
13. Sobin LH, Hermanek P and Hutter RV: TNM classification of malignant tumors. A comparison between the new (1987) and the old editions. Cancer 61: 2310-2314, 1988.
14. Hiyama K, Hiyama E, Ishioka S, Yamakido M, Inai K, Gazdar AF, Piatyszek MA and Shay JW: Telomerase activity in small-cell and non-small-cell lung cancers. J Natl Cancer Inst 87: 895-902, 1995.
15. Hiyama K, Ishioka S, Shirotani Y, Inai K, Hiyama E, Murakami I, Isobe T, Inamizu T and Yamakido M: Alterations in telomeric repeat length in lung cancer are associated with loss of heterozygosity in p53 and Rb. Oncogene 10: 937-944, 1995.
16. Mendoza C, Sato H, Hiyama K, Ishioka S, Isobe T, Maeda H, Hiyama E, Inai K and Yamakido M: Allelotype and loss of heterozygosity around the L-myc gene locus in primary lung cancers. Lung Cancer 28: 117-125, 2000.
17. Tanaka T, Tanimoto K, Otani K, Satoh K, Ohtaki M, Yoshida K, Toge T, Yahata H, Tanaka S, Chayama K, Okazaki Y, Hayashizaki Y, Hiyama K and Nishiyama M: Concise prediction models of anticancer efficacy of 8 drugs using expression data from 12 selected genes. Int J Cancer 111: 617-626, 2004.
18. Hiyama K, Tanimoto K, Nishimura Y, Tsugane M, Fukuba I, Sotomaru Y, Hiyama E and Nishiyama M: Exploration of the genes responsible for unlimited proliferation of immortalized lung fibroblasts. Exp Lung Res 34: 373-390, 2008.
19. Herman JG, Graff JR, Myohanen S, Nelkin BD and Baylin SB: Methylation-specific PCR: a novel PCR assay for methylation status of CpG islands. Proc Natl Acad Sci USA 93: 9821-9826, 1996.
20. Hiyama K, Hiyama E and Shay JW: Telomeres and telomerase in humans. In: Telomeres and Telomerase in Cancer. Hiyama K (ed.). Humana Press, Springer, New York, NY, pp3-21, 2009.
21. Hiyama E, Hiyama K, Yokoyama T and Shay JW: Immunohistochemical detection of telomerase (hTERT) protein in human cancer tissues and a subset of cells in normal tissues. Neoplasia 3: 17-26, 2001.
22. Kumazaki T, Hiyama K, Takahashi T, Omatsu H, Tanimoto K, Noguchi T, Hiyama E, Mitsui Y and Nishiyama M: Differential gene expressions during immortalization of normal human fibroblasts and endothelial cells transfected with human telomerase reverse transcriptase gene. Int J Oncol 24: 1435-1442, 2004.
23. Miyazu YM, Miyazawa T, Hiyama K, Kurimoto N, Iwamoto Y, Matsuura H, Kanoh K, Kohno N, Nishiyama M and Hiyama E: Telomerase expression in non-cancerous bronchial epithelia is a possible marker of early development of lung cancer. Cancer Res 65: 9623-9627, 2005.
24. Kraunz KS, Nelson HH, Lemos M, Godleski JJ, Wiencke JK and Kelsey KT: Homozygous deletion of $p16^{INK4a}$ and tobacco carcinogen exposure in nonsmall cell lung cancer. Int J Cancer 118: 1364-1369, 2006.
25. Yokota J and Kohno T: Molecular footprints of human lung cancer progression. Cancer Sci 95: 197-204, 2004.
26. Heppner GH: Tumor heterogeneity. Cancer Res 44: 2259-2265, 1984.
27. Lou H and Dean M: Targeted therapy for cancer stem cells: the patched pathway and ABC transporters. Oncogene 26: 1357-1360, 2007.

Advanced Drug Delivery Reviews 61 (2009) 402–407

Contents lists available at ScienceDirect

Advanced Drug Delivery Reviews

journal homepage: www.elsevier.com/locate/addr

Pharmacokinetics and pharmacogenomics in gastric cancer chemotherapy ☆

Masahiko Nishiyama *, Hidetaka Eguchi

Translational Research Center, Saitama Medical University International Medical Center, 1397-1 Yamane, Hidaka, Saitama 350-1298, Japan

ARTICLE INFO

Article history:
Received 19 September 2008
Accepted 27 September 2008
Available online 3 December 2008

Keywords:
Gastric cancer
Chemotherapy
Pharmacokinetics
Pharmacogenomics
Treatment optimization

ABSTRACT

Despite extensive efforts, treatment of gastric cancer by chemotherapy, the globally accepted standard, is yet undetermined, and uncertainty remains regarding the optimal regimen. Recent introduction of active "new generation agents" offers hope for improving patient outcomes. Current chemotherapeutic trials provided several regimens that may become a possible standard treatment, including docetaxel/cisplatin/5-FU (TCF) and cisplatin/S-1 for advanced and metastatic cancer and S-1 monotherapy in the adjuvant setting. Along with the development of novel active regimens, individual optimization of cancer chemotherapy has been attempted in order to reduce toxicity and enhance tumor response. Unlike the rare and limited contribution of pharmacokinetic studies, pharmacogenomic studies are increasing the potential to realize the therapeutics against gastric cancer. Despite the limited data, pharmacogenomics in gastric cancer have provided a number of putative biomarkers for the prediction of tumor response to chemotherapies and of toxicity.

© 2008 Elsevier B.V. All rights reserved.

Contents

1. Introduction

Gastric cancer is the fourth most common cancer and the second most frequent cause of cancer-related mortality worldwide, accounting for approximately 930,000 new cases and 700,000 deaths annually [1,2]. In gastric cancer, radical surgery remains the standard form of therapy that has curative intent, although chemotherapy has been intensively studied in a variety of settings as a most potent treatment option to improve the poor survival rate [3–5]. A series of trials has produced evidence that chemotherapy increases survival, but a globally accepted standard chemotherapy is yet undetermined, and uncertainty remains regarding the choice of the optimal regimen.

Recently, several active agents have been introduced to gastric cancer therapy: the taxanes, irinotecan (CPT-11), oxaliplatin, S-1, capecitabine, and, more recently, biological agents such as cetuximab and bevacizumab [3–7]. The advent of new regimens of these new generation agents offer hope for improving patient outcomes, and rapid advances in genomics present the opportunity to establish a novel chemotherapeutic strategy, personalized medicine, which would allow the selection of optimal therapy and dose for each

☆ This review is part of the *Advanced Drug Delivery Reviews* theme issue on "Recent advances in Cancer Chemotherapy: Current Strategies, Pharmacokinetics, and Pharmacogenomics".

* Corresponding author. Translational Research Center, Saitama Medical University International Medical Center, 1397-1 Yamane, Hidaka City, Saitama 350-1298, Japan. Tel.: +81 42 984 4668; fax: +81 42 984 4741.
E-mail addresses: yamacho@saitama-med.ac.jp (M. Nishiyama), eguchi@saitama-med.ac.jp (H. Eguchi).

0169-409X/$ - see front matter © 2008 Elsevier B.V. All rights reserved.
doi:10.1016/j.addr.2008.09.004

Table 1
Current chemotherapeutic option and supporting Phase III study in gastric cancer.

Treatment	Phase III study (Pts.No)	Main results
Neoadjuvant setting		
ECF [11]	MAGIC trial (503)	⊕ Higher PFS and higher likelihood of OS in ECF group (vs. surgery alone)
Adjuvant setting		
45 Gy radiation + 5-FU/FA [10]	INT-0116/SWOG 9008 study3 (556)	⊕ Higher RFS and OS in stage IB to stage IV (M0) patients underwent complete rsection (vs. surgery alone)
S-1 monotherapy [12]	ACTS-GC (1059)	⊕ Higher RFS and OS in stage II/III patients who underwent complete resection with D2 dissection vs. surgery alone) ⊕ Less Grade 3/4 toxicity than other regimens.
Metastatic stage		
TCF [17,18]	V-325 study	⊕ Higher RR, TTP and OS (vs. CF)
S-1 monotherapy [20]	JCOG 9912	⊕ Higher likelihood of OS to continuous 5-FU ⊖ Compatible OS with CPT-11/cisplatin and significant less Grade 3/4 toxicity
S-1/cisplatin [21]	SPIRITS trial	⊕ Higher PFS and OS (vs. S-1 monotherapy)

ECF, epirubicin/cisplatin/5-FU combination; TCF, doceraxel/cisplatin/5-FU combination; OS, overall survival; RFS, relapse-free survival; RR, response rate; TTP, time to tumor progression; PFS, progression-free survival.

individual based on molecular profiles of both the tumor and the patient [8,9].

2. Current chemotherapeutic strategies for gastric cancer

Although personalized medicine is an attractive strategy with great potential, at present, establishment of the first golden standard regimen takes priority over the development of novel therapeutics against gastric cancer. A great deal of effort has been directed towards development of the best regimen in various treatment settings (Table 1) [3–7].

2.1. Adjuvant chemotherapy

In the US, chemoradiation therapy (CRT) has been evaluated as the focus for an adjuvant treatment. The Phase III Intergroup trial (INT-0116/SWOG 9008 study3) is noteworthy among the conducted trials [10]. This study demonstrated that adjuvant 45 Gy radiation therapy with combined chemotherapy of 5-fluorouracil (5-FU) and folinic acid (FA) improved relapse-free survival (RFS) and overall survival (OS) in 556 patients with completely resected stage IB to stage IV (M0) adenocarcinoma of the stomach and gastroesophageal junction. Based on the results, CRT after potentially curative surgery for node-positive patients is now regarded as a standard treatment in the US.

Perioperative (pre- and post-operative) chemotherapy without radiation therapy has also been intensively studied. In UK, a large phase III study, The Medical Research Council Adjuvant Gastric Infusional Chemotherapy (MAGIC) trial, was conducted to evaluate the efficacy of ECF combination regimen (epirubicin, cisplatin, and continuous infusion of 5-FU) as a perioperative adjuvant therapy (before and after surgery) [11]. The study, in which 503 patients with stage II or higher adenocarcinoma of the stomach or of the lower third of the esophagus were enrolled, demonstrated a significantly higher progression-free survival (hazard ratio [HR] for progression, 0.66; 95% confidence interval [CI], 0.53–0.81; P<0.001) and OS (HR for death, 0.75; 95% CI, 0.60–0.93; P = 0.009) in the perioperative chemotherapy group compared with the group of patients who have undergone surgery alone. The study also validated the feasibility of the regimen in a preoperative adjuvant setting, which led to the current European recognition of neoadjuvant chemotherapy as a standard treatment option in gastric cancer. Neoadjuvant CRT remains under clinical evaluation.

The recent Phase III studies also supported the role of post-adjuvant chemotherapy in gastric cancer. The ACTS-GC conducted in Japan, in which a total of 1,059 patients were enrolled, evaluated the adjuvant efficacy of S-1 monotherapy compared with surgery alone, with OS as the primary end point, and showed the benefit of S-1 monotherapy as postoperative adjuvant chemotherapy for stage II/III patients who underwent D2 dissection [12]. Three-year OS after S-1 monotherapy was 81.1%, while that of the surgery alone group was 70.1% (P = 0.0015), and Grade 3/4 adverse events were less frequent than other regimens. RFSs after a 3-year follow-up of S-1 and of the surgery alone group were 72.2% and 60.1%, respectively (P = 0.0001). The feasible and effective adjuvant therapy with S-1 monotherapy after curative surgery is regarded as the standard of care of stage II/III gastric cancer patients in Japan. The Italian Gruppo Oncologico dell'Italia Meridionale (GOIM) study also found positive results for epirubicin/etoposide/5-FU/FA) in patients who underwent D1, D2 dissection [13].

2.2. Chemotherapy in advanced, metastatic, and recurrent gastric cancer

For advanced, metastatic, and recurrent gastric cancer, 5-FU- and/or cisplatin-based combinations remain the mainstay of treatment [3–7]. A meta-analysis by Wagner et al. showed that conventional cytotoxic chemotherapy (n = 103) can improve OS (HR = 0.39, 95%CI: 0.28–0.52, P<0.00001), quality of life (HR = 2.07, 95% CI: 1.31–3.28, P = 0.002) and symptom-free period (HR = 2.33, 95% CI: 1.41–3.87, P = 0.001) compared with Best Supportive Care (BSC) (n = 81). The analysis also demonstrated a survival benefit of cytotoxic combinations (n = 836) over single-agent (n = 636) chemotherapy (HR = 0.83, 95% CI: 0.74–0.93, P = 0.001) and an advantage of cisplatin based on OS [14]. Indeed, both CF (cisplatin/5-FU) and ECF (epirubicin/cisplatin/5-FU) are regarded as the most potent treatment option in various countries, especially in the US and Europe.

Nevertheless, with these "classical" combinations, median survival time (MST) does not exceed 7-10 months. Current studies have focused on "new generation agents," such as the taxanes (paclitaxel and docetaxel), irinotecan, oxaliplatin, new oral fluoropyrimidines, and biological agents [3–7]. Several combinations of these agents, with response rates of up to 65% reported in phase II studies, have been investigated in randomized phase II/III studies [15,16].

To date, docetaxel combinations, especially a docetaxel/cisplatin/5-FU (TCF) regimen, are likely crucial in various regimens. In the phase III V-325 study, the triple agent therapy was superior to CF in terms of response rate (37% vs. 25%; 95% CI: 30.3-43.4 vs. 19.9-31.7, chi-square P = 0.0106), time to progression (TTP; 5.6 months vs. 3.7 months; HR = 1.47, 95% CI: 1.19–1.82, risk reduction 32%, log-rank P = 0.0004), and survival (risk reduction 23%, HR = 1.29, 95% CI: 1.0–1.6, log-rank P = 0.0201) in patients with metastatic gastric cancer [17,18]. TCF triplet is recognized as a new reference regimen for advanced gastric cancer in the US and Europe. However, the triplet regimen appeared to be highly toxic compared with other regimens. The optimizing studies of the original regimen, in terms of both the efficacy and safety, are currently in progress [19].

New oral 5-FU analogs and prodrugs such as S-1 and capecitabine are also attractive alternative agents for combination with other anticancer agents. Recent phase III trials have focused on the use of oral 5-FU, especially for S-1, and demonstrated these pivotal activities. A three arm Phase III study [Japan Clinical Oncology Group (JCOG) 9912]